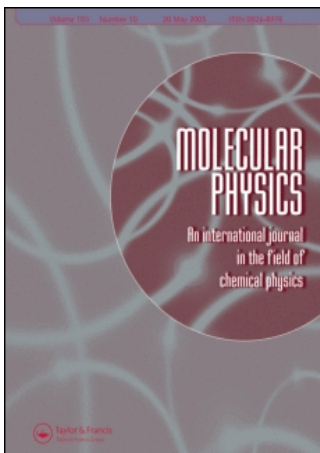


This article was downloaded by:[Prisner, T. F.]  
On: 18 December 2007  
Access Details: [subscription number 788607874]  
Publisher: Taylor & Francis  
Informa Ltd Registered in England and Wales Registered Number: 1072954  
Registered office: Mortimer House, 37-41 Mortimer Street, London W1T 3JH, UK



## Molecular Physics

### An International Journal in the Field of Chemical Physics

Publication details, including instructions for authors and subscription information:  
<http://www.informaworld.com/smpp/title~content=t713395160>

#### Conformational flexibility of nitroxide biradicals determined by X-band PELDOR experiments

D. Margraf<sup>a</sup>; B. E. Bode<sup>a</sup>; A. Marko<sup>a</sup>; O. Schiemann<sup>a</sup>; T. F. Prisner

<sup>a</sup>Institute of Physical and Theoretical Chemistry and Center of Biomolecular Magnetic Resonance, J.W. Goethe University, Frankfurt am Main 60438, Germany

Online Publication Date: 01 August 2007

To cite this Article: Margraf, D., Bode, B. E., Marko, A., Schiemann, O. and Prisner, T. F. (2007) 'Conformational flexibility of nitroxide biradicals determined by X-band PELDOR experiments', *Molecular Physics*, 105:15, 2153 - 2160

To link to this article: DOI: 10.1080/00268970701724982

URL: <http://dx.doi.org/10.1080/00268970701724982>

PLEASE SCROLL DOWN FOR ARTICLE

Full terms and conditions of use: <http://www.informaworld.com/terms-and-conditions-of-access.pdf>

This article maybe used for research, teaching and private study purposes. Any substantial or systematic reproduction, re-distribution, re-selling, loan or sub-licensing, systematic supply or distribution in any form to anyone is expressly forbidden.

The publisher does not give any warranty express or implied or make any representation that the contents will be complete or accurate or up to date. The accuracy of any instructions, formulae and drug doses should be independently verified with primary sources. The publisher shall not be liable for any loss, actions, claims, proceedings, demand or costs or damages whatsoever or howsoever caused arising directly or indirectly in connection with or arising out of the use of this material.

# Conformational flexibility of nitroxide biradicals determined by X-band PELDOR experiments

D. MARGRAF, B. E. BODE, A. MARKO, O. SCHIEMANN and T. F. PRISNER\*

Institute of Physical and Theoretical Chemistry and Center of Biomolecular Magnetic Resonance, J.W. Goethe University, Max-von-Laue-Str. 7, Frankfurt am Main 60438, Germany

(Received 12 June 2007; in final form 28 September 2007)

PELDOR (pulsed electron–electron double resonance) experiments have been performed at X-band (9 GHz) frequencies on a linear and a bent nitroxide biradical. All PELDOR time traces were recorded with the pump frequency  $\nu_B$  set at the center of the nitroxide spectra to achieve maximum pumping efficiency, while the probe frequency  $\nu_A$  was stepped between a frequency offset  $\Delta\nu_{AB} = \nu_A - \nu_B$  of +40 to +80 MHz. The modulation frequencies and the damping of the oscillations change as a function  $\Delta\nu_{AB}$ , whereas the modulation depth  $\lambda$  for our investigated systems was only very slightly altered. This can be explained by the selection of different orientations of nitroxide radicals with respect to the external magnetic field as a function of frequency offset. Quantitative simulations of the PELDOR time traces could be achieved for both molecules and for all offset frequencies using a simple geometric model, described by a free rotation of the nitroxide radical around its acetylene bond and a single bending mode of the interconnecting molecular bridge. The results show that the distribution function for the relative orientations of the nitroxides with respect to each other and with respect to the dipolar vector  $\mathbf{R}$  deviates from a random distribution and thus has to be taken into account to quantitatively simulate the PELDOR traces. *Vice versa*, a quantitative simulation of PELDOR time traces with variable offset frequencies allows the determination of the conformational freedom of such molecules.

*Keywords:* PELDOR; DEER; EPR; ESR; Nitroxide

## 1. Introduction

PELDOR [1] is a powerful tool for measuring the distances between paramagnetic centres in the nanometer range [2]. The method has been widely applied to measure distances in spin-labeled macromolecules such as polymers [3] and biomolecules [4]. The method uses the magnetic dipole–dipole interaction to probe the distance in analogy to FRET spectroscopy, where the electric dipole–dipole interaction is utilized. In both methods, not only the distance, but also the orientation of the two dipoles with respect to the interconnecting distance vector  $\mathbf{R}$  between the two radical centres affects the coupling strength. Nitroxides, which are commonly used as spin labels, typically have a large rotational and conformational freedom. Therefore, in most studies the relative orientation has been considered as random, leading to the well known Pake pattern distribution of dipolar coupling strengths. In such cases the most

prominent coupling strength corresponds to an orientation where the  $\mathbf{R}$ -vector is perpendicular to the external magnetic field. The peak resulting from the perpendicular orientation of the  $\mathbf{R}$ -vector with respect to the external magnetic field is usually chosen in order to determine the distance between the two radicals. Observation of the full Pake pattern by a four-pulse PELDOR sequence [5] (figure 1) allows the disentanglement of the orientation-dependent dipolar coupling  $D(\theta_{\text{dip}})$  from the isotropic exchange coupling  $J$ , which additionally may occur for distances smaller than 2 nm [6].

In cases where the orientation of the radicals to the interconnecting vector  $\mathbf{R}$  is fixed, such as, for example, for natural paramagnetic cofactors in proteins, a different situation arises if specific orientations of the radicals can be selected by the resonant microwave pulses. Here, the orientation of the radicals with respect to the  $\mathbf{R}$ -vector enters into the analysis. The observed coupling strength and the modulation depth  $\lambda$  as well as the attenuation of the dipolar oscillations will depend on the specific choice of the probe and the pump frequencies

\*Corresponding author. Email: prisner@prisner.de

[2]. Especially at high magnetic field values, where the  $g$ -tensor anisotropy of the radicals is usually resolved, such orientation selectivity can readily be achieved [7], as has been demonstrated for two tyrosyl radicals in a ribonucleotide reductase dimer at G-band frequencies (180 GHz/6.5 T). In this case, a strong orientation dependence of the experimentally observed dipolar oscillation frequency could be observed, permitting to additionally obtain the relative orientation of the tyrosyl radicals with respect to the  $\mathbf{R}$ -vector [8].

Such orientation selection and angular correlation effects have already been observed in nitroxide biradicals with polyphenyleneethynylene linkers at X-band (9 GHz/0.3 T) [9], S-band (3 GHz/0.1 T) [6] and W-band (95 GHz/3.4 T) [10] frequencies.

In this paper, we show that these orientation effects can be quantified by  $\Delta\nu_{AB}$ -dependent PELDOR measurements at X-band frequencies. A quantitative numerical simulation of the PELDOR time traces recorded as a function of  $\Delta\nu_{AB}$  can be used to derive distinct information on the conformational flexibility of such molecules.

## 2. Theory

The magnetic dipole–dipole interaction between the magnetic moments  $\mu_A$  and  $\mu_B$  of two paramagnetic centres leads to an interaction energy  $E$  of

$$E = \frac{\mu_A \cdot \mu_B}{R^3} - \frac{3(\mu_A \cdot \mathbf{R})(\mu_B \cdot \mathbf{R})}{R^5}, \quad (1)$$

where  $\mathbf{R}$  is the distance vector A and B. In the secular approximation, the dipolar Hamiltonian  $H_{\text{dip}}$  can be written in the following way:

$$H_{\text{dip}} = \frac{g_A g_B \beta_e^2}{R^3} S_z^A S_z^B (1 - 3 \cos^2 \theta_{\text{dip}}), \quad (2)$$

with  $g_A$  and  $g_B$  being the  $g$ -values of the paramagnetic molecules A and B,  $\beta_e$  the Bohr magneton,  $\mathbf{R}$  the distance between the two molecules and  $\theta_{\text{dip}}$  the angle between the

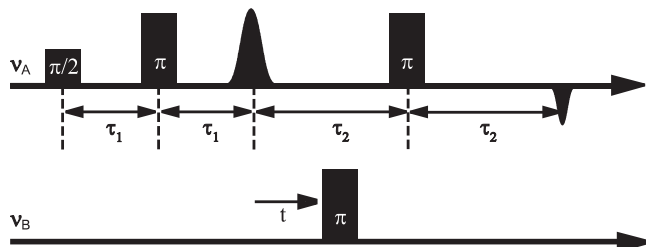


Figure 1. The four-pulse PELDOR sequence used for these measurements. The variable time  $t$  of the pump pulse is zero at the first Hahn-echo position.

external magnetic field  $B_0$  and the  $\mathbf{R}$ -vector. The dipolar splitting of the EPR transitions is therefore given by

$$\omega_{\text{dip}} = \frac{D_{\text{dip}}}{R^3} (1 - 3 \cos^2 \theta_{\text{dip}}), \quad (3)$$

where the splitting constant  $D_{\text{dip}}$  is  $2\pi \cdot 52 \text{ MHz nm}^3$  for nitroxide radicals. The  $\mathbf{R}$ -vectors in a macroscopically disordered frozen solution sample are randomly oriented with respect to the external magnetic field. As can be seen from equation (3),  $\omega_{\text{dip}}$  varies from  $-2D_{\text{dip}}/R^3$  to  $+D_{\text{dip}}/R^3$ . If all molecules are excited, the amplitude of this dipolar frequency distribution is described by the classical Pake pattern [11]. The edge-to-edge distance of the Pake pattern corresponds to the dipolar splitting for molecules with an angle of  $\theta_{\text{dip}} = 0^\circ$  between the  $\mathbf{R}$ -vector and the external magnetic field  $B_0$ , the peak-to-peak distance to the dipolar splitting for molecules with  $\theta_{\text{dip}} = 90^\circ$ . These two peaks are the most prominent observable features in Fourier-transformed four-pulse PELDOR time traces [12].

The echo intensity  $V(t)$  of a four-pulse PELDOR sequence for a fixed orientation of the magnetic field  $B_0$  in the A spin molecular axis system (described by polar angles  $\varphi$  and  $\phi$ ) is given by:

$$V(t, \nu_A, \nu_B, \varphi, \phi) = V_0(\nu_A, \varphi, \phi) \cdot (1 - \lambda(\nu_B, \Omega, \varphi, \phi) \cdot [1 - \cos(\omega_{\text{dip}}(\varphi, \phi) \cdot t)]), \quad (4)$$

where  $V_0$  describes the A spin echo intensity for  $t=0$ ,  $\Omega$  is the set of Euler angles describing the orientation of spin B in the axis system of spin A (figure 2) and  $\lambda$  is the efficiency of inversion of the dipolar coupled spin B by the pump pulse. For disordered powder samples the observed echo intensity is obtained by integration over all magnetic field orientations:

$$V(t, \nu_A, \nu_B) = \iint V(t, \nu_A, \nu_B, \varphi, \phi) \sin(\phi) d\phi d\varphi. \quad (5)$$

The relative orientation between spin A and B as well as with respect to the vector  $\mathbf{R}$  will all be random regarding

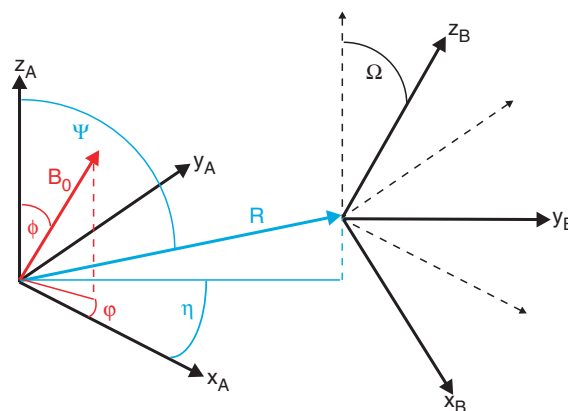


Figure 2. Definition of the axis system of biradicals 1 and 2.

flexible biradicals. In such cases, integration over all  $\Omega$  values will effectively average the magnetic field orientation dependence of the modulation depth parameter  $\lambda$  [13]. Hence, the integration over the different magnetic field orientations of equation (5) can readily be converted into an integration over all dipolar angles:

For more rigid biradicals this simplification is not valid. The pump efficiency, described by the modulation

$$V(t, \nu_A, \nu_B) = V_0(\nu_A) \cdot \left( 1 - \lambda(\nu_B) \cdot \left[ 1 - \int_0^{\pi/2} \cos\left(\frac{D_{\text{dip}}}{R^3}(1 - 3\cos^2\theta_{\text{dip}})t\right) \sin\theta_{\text{dip}} d\theta_{\text{dip}} \right] \right). \quad (6)$$

depth parameter  $\lambda$ , will depend on the mutual orientation of the two radicals A and B, described by the Euler angles  $\Omega$ . Additionally, the orientation selectivity of the excitation of spin A as a function of  $\nu_A$ , described by  $V_0(\nu_A, \varphi, \phi)$ , will lead to a distribution function  $P(\nu_A, \theta_{\text{dip}})$  of dipolar angles that differs from the  $\sin(\theta_{\text{dip}})$  distribution of a Pake pattern. The echo signal intensity for a given pump and probe frequency can, in such general cases, be described by [2, 13]:

Thus, the observed dipolar frequency spectrum cannot be converted directly into a distance  $R$  if the

$$V(t, \nu_A, \nu_B) = V_0(V_A) \left( 1 - \int_0^{\pi/2} P(\Delta\nu_{AB}, \theta_{\text{dip}}) \cdot [1 - \cos(\omega_{\text{dip}} \cdot t)] d\theta_{\text{dip}} \right). \quad (7)$$

$$\begin{aligned} \nu_{\text{res}}^A &= \beta_e \cdot B_0 \cdot g_{\text{eff}}^A + m_I \cdot A_{\text{eff}}^A, \\ g_{\text{eff}}^A &= \sqrt{(g_{xx} \cdot \cos\varphi \cdot \sin\phi)^2 + (g_{yy} \cdot \sin\varphi \cdot \sin\phi)^2 + (g_{zz} \cdot \cos\phi)^2}, \\ A_{\text{eff}}^A &= \sqrt{(A_{xx} \cdot \cos\varphi \cdot \sin\phi)^2 + (A_{yy} \cdot \sin\varphi \cdot \sin\phi)^2 + (A_{zz} \cdot \cos\phi)^2}, \end{aligned} \quad (8)$$

geometry of the biradical, and therefore the function  $P(\nu_A, \theta_{\text{dip}})$ , is unknown. To unravel orientation and distance information in such cases, the excitation and pump frequencies have to be varied to excite and pump differently oriented sub-ensembles of the powder sample.

For flexible biradicals, with a statistical distribution of orientations, the time domain PELDOR traces, as described by equation (6), can easily be simulated by Tikhonov regularization methods [14]. However, it is more demanding for conformationally restricted biradicals, because the integral kernel function of the integral in equation (7) is more complicated. We have therefore chosen a different strategy to simulate the experimental PELDOR time traces: a conformational ensemble of biradicals is created and their calculated

PELDOR time traces are compared with experiments. The conformational ensemble contains a number  $N$  (typically 1000 to 10 000) of different conformers, each characterized by a distance vector  $\mathbf{R}$ , with polar angles  $(\psi, \eta)$  in the axis system of spin A, and Euler angles  $\Omega$  describing the mutual orientation of molecule B with respect to molecule A. The input data for the structure of the conformers can be generated either by

molecular dynamics (MD) studies or by a simple geometrical model of the biradical. For each of these conformers the resonance positions of molecules A and B are calculated for all orientations of the magnetic field vector  $B_0$  in the molecular axis frame of spin A, taking anisotropic nitrogen hyperfine coupling and the anisotropy of the  $g$ -tensor into account:

where  $A_{\text{eff}}$  and  $g_{\text{eff}}$  are the effective hyperfine couplings and  $g$ -values for the specific magnetic field orientation, and  $m_I$  is the nuclear spin value ( $-1, 0, +1$  for  $^{14}\text{N}$ ). The

hyperfine and  $g$ -tensor axes are considered as collinear to the molecular axis system for our simulations. The resonance frequencies of spin B can be calculated after describing the hyperfine and  $g$ -tensor of spin B in the coordinate system of spin A, as given by the transformation

$$\begin{aligned} G_B^A &= D(\Omega) G_B^B D^{-1}(\Omega), \\ A_B^A &= D(\Omega) A_B^B D^{-1}(\Omega), \end{aligned} \quad (9)$$

where  $D(\Omega)$  is the respective rotation matrix. Additionally, an inhomogeneous linewidth of 0.6 mT has been taken into account by a Gaussian distribution to calculate the final resonance frequencies for spin A and spin B, respectively.

Using these calculated resonance frequencies the excitation efficiency of pump and probe pulses for spins A and B can easily be determined. For a microwave pulse with a Rabi oscillation frequency  $\omega_1 = \gamma B_1$  and a resonance frequency  $\Delta\omega_r = 2\pi(\nu_{mw} - \nu_{res})$ , the inversion efficiency is given by

$$I_{ex}(\Delta\omega_r, \varphi, \phi) = \left( \frac{1}{2} - \frac{\Delta\omega_r^2 + \omega_1^2 \cdot \cos[\pi(\Delta\omega_r^2 + \omega_1^2)^{1/2}/\omega_1]}{2(\Delta\omega_r^2 + \omega_1^2)} \right). \quad (10)$$

For a large sample size the inhomogeneous field strength  $B_1$  distribution over the resonator height can be described by a half sine-wave. Integration of equation (10) over the resonator length leads to an excitation profile that can be approximated by

$$I_{ex}(\Delta\omega_r, \varphi, \phi) = \frac{\omega_1^2}{\omega_1^2 + 4 \cdot \Delta\omega_r^2}. \quad (11)$$

This allows the calculation of the excitation functions of spin A,  $V_0(\nu_A, \varphi, \phi)$ , and of spin B,  $\lambda(\nu_B, \Omega, \varphi, \phi)$ , and thereafter the dipolar distribution function  $P(\nu_A, \theta_{dip})$  for each conformer. The pump pulse frequency  $\nu_B$  is fixed to the centre of the nitroxide spectrum in our experiments and only the detection frequency  $\nu_A$  is varied. The final PELDOR signal for a given frequency offset  $\Delta\nu_{AB}$  is the sum over all magnetic field orientations equally distributed on a sphere (typically 20 000) and over all conformers. All simulations are performed with a laboratory-written MATLAB<sup>®</sup> program. A simulation of an ensemble of 1000 conformers, each of them with 20 000 orientations with respect to the magnetic field, takes about 3 min of computing time on a personal computer.

### 3. Samples and experimental conditions

Biradicals **1** and **2** (figure 3) were synthesized according to the literature [15]. Samples were prepared as 50  $\mu$ M solutions in toluene and degassed via several freeze-thaw cycles prior to storage in liquid nitrogen. PELDOR spectra were recorded on a Bruker ELEXSYS E580 pulsed X-band EPR spectrometer with a standard flex line probehead housing a dielectric ring resonator (MD5 W1) equipped with a continuous-flow helium cryostat (CF935) and temperature-control system (ITC 502), both from Oxford Instruments. The second microwave frequency was coupled into the microwave bridge by a commercially available setup (E580-400U) from Bruker. All pulses were amplified via a pulsed travelling wave tube (TWT) amplifier (117X) from Applied Systems Engineering. Over-coupling of the resonator led to a quality factor  $Q$  of about 100. Four-pulse PELDOR experiments were performed with the pulse sequence  $\pi/2(\nu_A) - \tau_1 - \pi(\nu_A) - (\tau_1 + t) - \pi(\nu_B) - (\tau_2 - t) - \pi(\nu_A) - \tau_2$ -echo. The excitation bandwidths of the pump and probe pulses have to be chosen small enough to avoid spectral overlap. On the other hand, the excitation width of the inversion pump pulse should be as large as possible to achieve a deep modulation depth  $\lambda$ , given by the fractions of spins B inverted by the pump pulse. Therefore, the pump pulse ( $\nu_B$ ) was set to 12 ns at the resonance frequency of the resonator and applied to the maximum of the nitroxide spectrum. The pulse amplitude was then optimized to the maximum inversion of a Hahn-echo on the pump frequency  $\nu_B$ . For the simulations, a pulse length of 16 ns had to be chosen to obtain the observed modulation depth  $\lambda$ . The difference might result from non-rectangular pulse

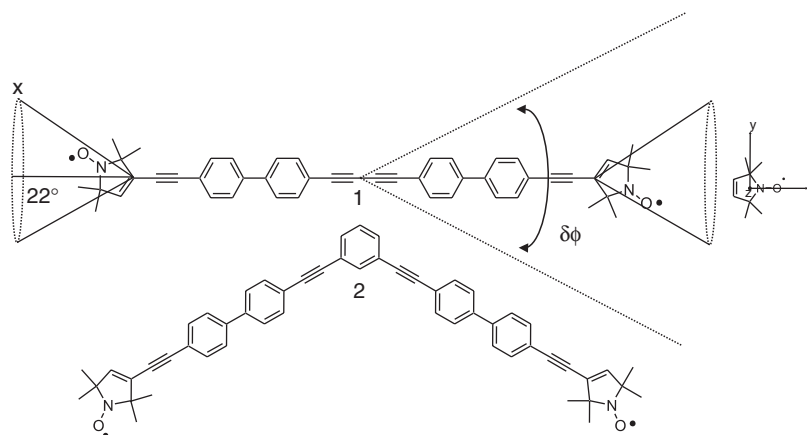


Figure 3. Structures of the two molecules **1** and **2** used in the experiments. The geometric model used to create an ensemble of conformers for these biradicals and the molecular axis system are indicated. The nitroxide radicals are assumed to rotate freely around their acetylene bond (cone with angle  $22^\circ$ ) and the mobility of the bridge is described by a single bending motion with a Gaussian distributed width  $\delta\phi$ .

shapes, the experimental reproducibility of  $\lambda$  or the adjustment of the optimum pulse lengths. Detection pulses ( $\nu_A$ ) were set to 32 ns and applied at frequency offsets  $\Delta\nu_{AB} = \nu_A - \nu_B$  from +40 to +80 MHz in 10 MHz steps with constant  $\nu_B$ . The pulse amplitudes were chosen to optimize the refocused echo and the  $\pi/2$  pulse was phase-cycled to eliminate receiver offsets. All spectra were recorded at 40 K with an experiment repetition time of 4 ms, a video amplifier bandwidth of 25 MHz and an amplifier gain of 60 dB.  $\tau_1$  was set to 136 ns and  $\tau_2$  to 4000 ns. Suppression of proton modulation was achieved by the addition of eight spectra of variable  $\tau_1$  with a  $\Delta\tau_1$  of 8 ns [16]. Usually, 720 scans were accumulated with 332 data points and time increments  $\Delta t$  of 12 ns, giving an approximate measurement time of 2 h. Intermolecular contributions to the time domain signal were removed by division by a mono-exponential decay. The resulting time traces were normalized to  $t=0$ .

#### 4. Results

Figure 4 shows the experimental PELDOR time traces for **1** and **2** as a function of the probe frequency offset  $\Delta\nu_{AB}$  ranging from 40 to 80 MHz. The pumping frequency  $\nu_B$  is, for all experiments, kept at the centre of the nitroxide spectra, as shown in the inset of figure 4. As can be seen, the oscillation frequencies vary as a function of  $\Delta\nu_{AB}$ . This indicates the presence of angular correlation effects for **1** and **2**. For the 80 MHz offset, a

high orientation selectivity for the observer spin A is obtained with our chosen pulse lengths; only nitroxide molecules with the plane normal almost parallel to the external magnetic field are observed, whereas for an offset of 40 MHz the orientation distribution of the excited nitroxides is broader. This is illustrated in figure 5: the contribution to the signal is encoded in colour for each orientation of the external magnetic field with respect to the nitroxide molecular axis system. Pumping in the centre of the nitroxide spectra with a 12 ns  $\pi$ -pulse length excites all molecular orientations. Only nitroxide molecules with the plane normal parallel to the external magnetic field and in the  $^{14}\text{N}$  nuclear  $m_I = \pm 1$  spin states (with a large hyperfine coupling) are not excited. For the linear biradical **1**, where the molecular  $z$  axis of the two nitroxides is perpendicular to the  $\mathbf{R}$ -vector (considering a rigid molecule), this

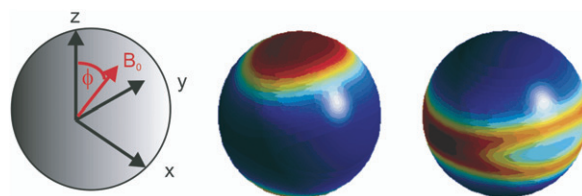


Figure 5. Calculated orientation selection for a nitroxide radical with  $\Delta\nu_{AB} = 80$  MHz (left) and  $\Delta\nu_{AB} = 40$  MHz (right). A pulse length of 32 ns and an inhomogeneous linewidth of 6 G is used for the simulations. The colour code gives the intensity of the excitation efficiency (increasing from blue to red).

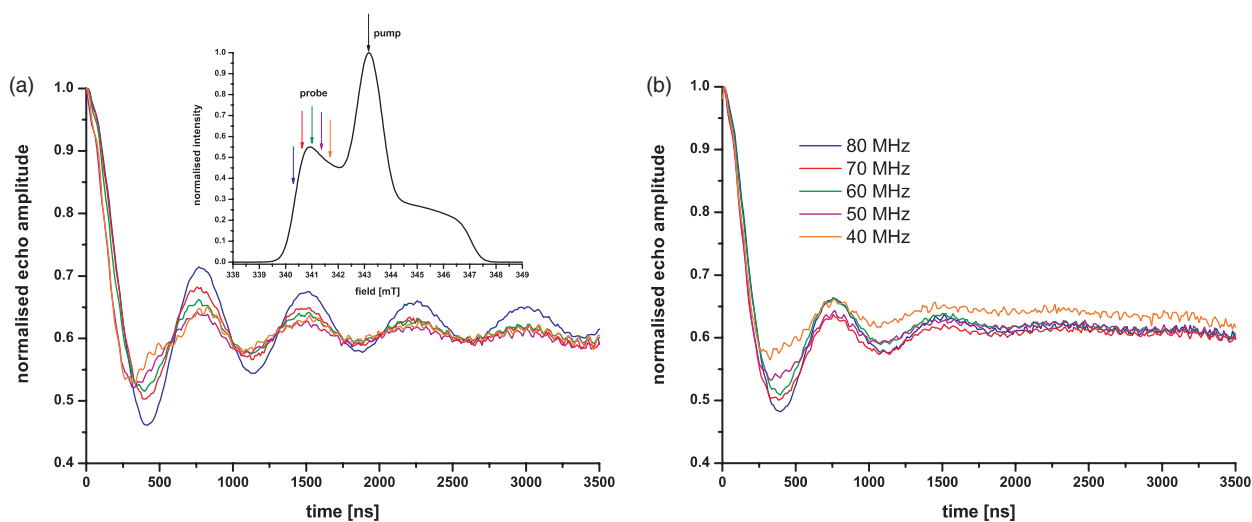


Figure 4. Experimental PELDOR time traces for offset frequencies  $\Delta\nu_{AB}$  between 40 and 80 MHz for molecules **1** (a) and **2** (b). All time traces are normalized to 1 for  $t=0$  and the intermolecular decay is removed by division by a mono-exponential decay, which is determined by fitting the experimental time traces for long  $t$  values. Inset: field swept EPR spectra of the nitroxide with the position of pump and probe frequencies indicated by arrows.

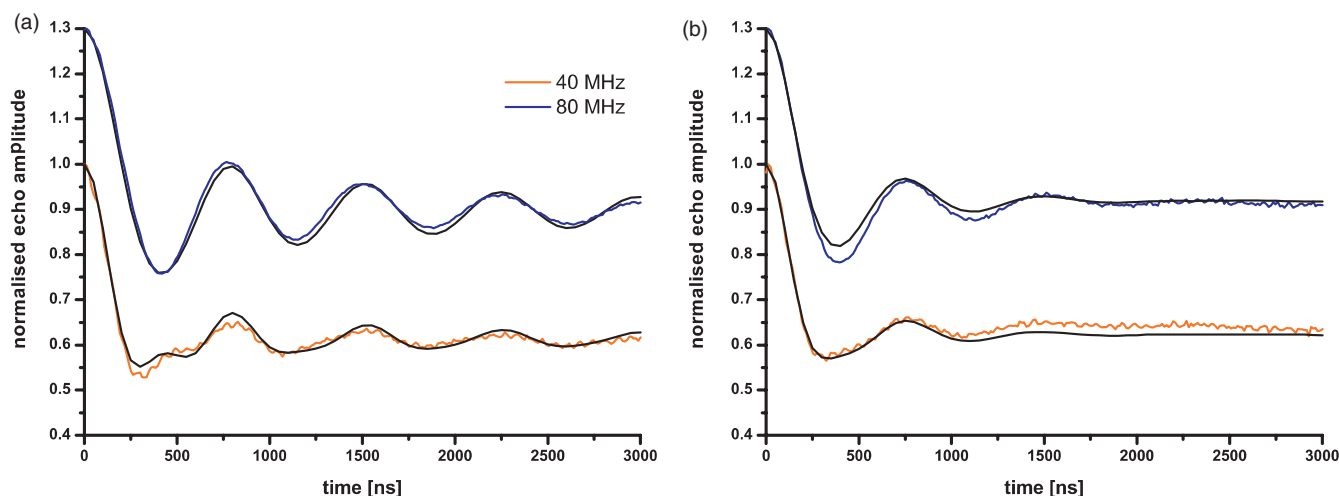


Figure 6. Simulated PELDOR time traces for **1** (a) and **2** (b) for  $\Delta\nu_{AB}=80$  MHz (blue, the normalized trace in the graph was shifted by  $+0.3$  in the  $y$  direction for better visibility) and  $\Delta\nu_{AB}=40$  MHz (orange). Simulations are shown in black. Parameters for the conformational distribution used for the simulation are given in the text.

orientation selection leads to simple predictions for the observable dipolar frequencies: the parallel frequency component should only appear for small frequency offsets  $\Delta\nu_{AB}$ , whereas, at 80 MHz, with high orientation selection, only the perpendicular component of the Pake pattern should be observable. This tendency is observed experimentally, as shown in figure 4. On the other hand, the modulation depth  $\lambda$  does not change as a function of  $\Delta\nu_{AB}$  for **1** and **2**. Also for the bent biradical **2**, a change of oscillation frequency is observed as a function of  $\Delta\nu_{AB}$  (figure 4(b)). The effect is less pronounced compared with **1** because, for **2**, a much faster damping of the oscillations occurs.

## 5. Discussion

The simple geometric model that we applied to simulate the conformational distribution of the biradicals is shown in figure 3. The five-ring nitroxide molecules are allowed to rotate freely around their acetylene bond axis. This leads to a random orientation of the nitroxide  $x$  axis (N–O) on a cone with an angle of  $22^\circ$  with respect to the linear acetylene linker. The nitroxide  $z$  axis (out of plane) is perpendicular to the linear linker, but otherwise randomly oriented. The conformational flexibility of the interconnecting molecular bridge is modelled by a simple bending motion, as depicted in figure 3, with a Gaussian half width angle  $\delta\phi$ . The highest orientation selection and symmetry is achieved for molecule **1** with a frequency offset of 80 MHz. Under these conditions, only nitroxide radicals with the normal parallel to the external magnetic field contribute to the signal. The bending angle  $\delta\phi$  was optimized on the basis of

this experimental data set. The best result was obtained with a bending angle of  $\delta\phi=40^\circ$ . With the same conformational distribution, the frequencies, modulation depth and attenuation of the PELDOR traces obtained with other frequency offsets could also be well reproduced, as shown in figure 6 for  $\Delta\nu_{AB}=80$  MHz and 40 MHz. In particular, the damping and modulation depth can be compared much better with a simulation of the time domain data instead of the often used frequency domain data. The attenuation of the oscillations is strongly influenced by the bending angle  $\delta\phi$ . A quantitative reproduction of the experimentally observed attenuation of the oscillations can only be achieved by taking into account this relatively strong bending. The large conformational freedom of the molecular bridge is in qualitative agreement with unpublished MD predictions and published MD studies [10, 17]. The MD and the simple conformational model both lead to a slightly shorter average distance than the predicted minimum energy structure and therefore a faster oscillation period, in agreement with the experimental data. Nevertheless, even with this fairly large flexibility of the bridge, orientation correlations exist, evident from the changes in oscillation frequencies for the smaller offset frequency of 40 MHz. Another factor that could alter the shape of the PELDOR traces with varying frequency offset is the spectral overlap between pump and probe pulses. The most prominent effect is that the short pump pulse also interacts with A spins excited by the probe pulse echo sequence. These A spins will no longer refocus at the echo position and therefore do not contribute to the PELDOR signal. Indeed, switching on the pump pulse leads to an experimentally observed reduction in echo intensity.

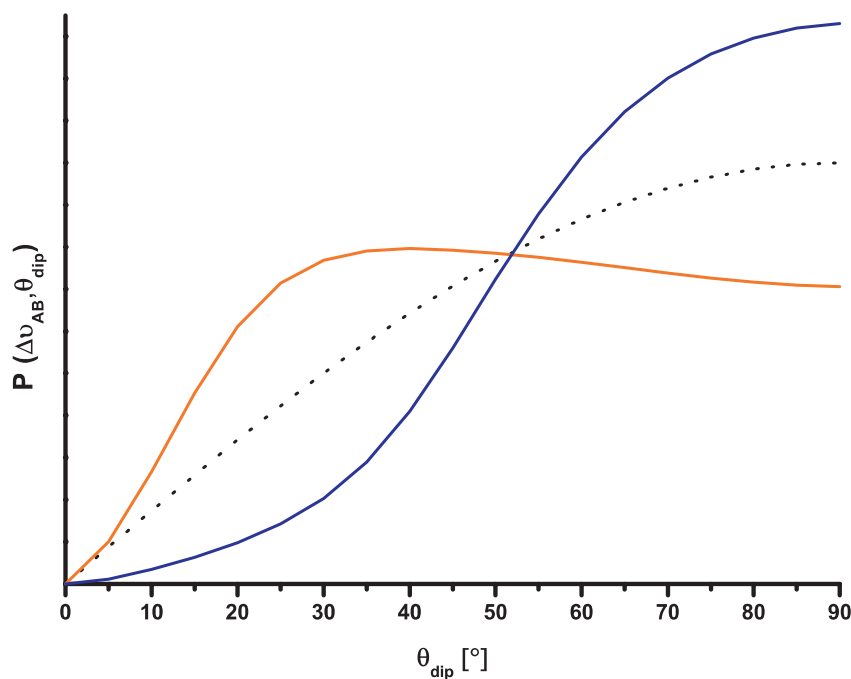


Figure 7. The function  $P(\Delta\nu_{AB}, \theta_{\text{dip}})$  describing the relative intensities of the dipolar frequencies contributing to the PELDOR signal of a disordered powder sample for two offset frequencies  $\Delta\nu_{AB} = 80$  MHz (blue) and  $\Delta\nu_{AB} = 40$  MHz (orange) normalised for comparison. For the simulation, the geometric model of biradical **1** as defined in the text was used. The black line shows the expected  $\sin(\theta_{\text{dip}})$  intensity for a biradical without any angular correlations, corresponding to a Pake pattern.

Simulation of this interference effect for  $\Delta\nu_{AB} = 40$  MHz also showed a reduction in echo intensity for the studied conformer ensemble, but no change in the PELDOR time trace shape within the experimental accuracy. This effect will be smaller for larger offset values, indicating that it does not contribute to the offset-dependent change in oscillation frequencies for the chosen experimental conditions.

Thus, the observed change in oscillation frequency as a function of  $\Delta\nu_{AB}$  can be attributed to the different selection of dipolar angles in both experiments. Figure 7 depicts the dipolar angle distribution function  $P(\Delta\nu_{AB}, \theta_{\text{dip}})$  for **1** extracted from the simulations for  $\Delta\nu_{AB} = 40$  MHz and 80 MHz. Both distributions deviate strongly from the  $\sin \theta_{\text{dip}}$  distribution expected for random orientations of the nitroxides with respect to the bridge. Whereas the distribution for  $\Delta\nu_{AB} = 80$  MHz is mainly located around  $\theta_{\text{dip}} = 90^\circ$ , smaller dipolar angles also contribute to the simulations with 40 MHz frequency offset. In particular, values close to  $\theta_{\text{dip}} = 0^\circ$  lead to the additional faster oscillations seen in this time trace.

For biradical **2**, with an angle of  $120^\circ$  in the bridge, the same conformational model, with a free rotation of the nitroxides around the acetylene linker bond and a single bending distribution  $\delta\phi$ , was used to simulate the PELDOR time traces. We could reproduce the experimental PELDOR time traces for all offset frequencies

well with a smaller mobility of the bridge of  $\delta\phi = 20^\circ$ . Simulations and experimental data are summarized in figure 6 for 80 MHz and 40 MHz frequency offsets. The much faster damping of the oscillations is a consequence of the angle in the bridge. The bending motion causes a much more pronounced effect on the distance in this case, leading to a broader distance distribution and therefore faster damping of the oscillations. This might also explain the slightly smaller angle  $\delta\phi$  for this molecule: in our simple model, where the conformational freedom of the bridge is approximated by only a single bending motion, the distance variation is obviously underestimated for the linear biradical **1**.

In both cases, we demonstrated that X-band PELDOR time traces are very sensitive to the conformational freedom of the biradical, and, in both cases, cannot be described accurately by a random orientation of the nitroxide radicals with respect to the molecular bridge. Both molecules can be reasonably well simulated by applying a simple geometric model.

## 6. Conclusion

We were able to show with a set of two biradicals that the  $\Delta\nu_{AB}$  dependence of the oscillation frequencies arises from orientation correlations between the nitroxides and the distance vector  $\mathbf{R}$ . Even with large

bending motions of the bridge, such effects may remain and hamper the analysis of the distance  $R$  between the two unpaired electrons. If the experiment is performed only with one fixed offset frequency and analysed by assuming a random orientation distribution, a wrong  $R$  distribution could result. This can be avoided by taking PELDOR time traces with different pump and probe frequencies. Summing all these time traces may lead to an averaging of such orientation correlations, as has been shown by Godt *et al.* [9]. On the other hand, a quantitative analysis of the frequency offset dependence will allow us to construct a detailed picture of the conformational distribution of the molecule. An analogous situation might also arise in biological applications where steric constraints restrict the mobility of the spin labels. By a systematic variation of the detection frequency  $\nu_A$ , such effects can easily be detected and taken into account. This yields additional information on the mutual orientation of the two nitroxide radicals, which might be interesting in structural studies.

Together with PELDOR experiments at different magnetic field values and under different freezing conditions, such experiments will generate benchmark data for optimization of the MD force field parameters and potentials for such molecules, as will be shown in a forthcoming publication.

## References

- [1] (a) A. D. Milov, K. M. Salikov, and M. D. Shirov, *Fiz. Tverd. Tela* **23**, 975 (1981). (b) A. D. Milov, A. B. Ponomarev, and Y. D. Tsvetkov, *Chem. Phys. Lett.* **110**, 67 (1984).
- [2] R. G. Larsen and D. J. Singel, *J. Chem. Phys.* **98**, 5134 (1993).
- [3] G. Jeschke, *Macromol. Rapid Commun.* **23**, 227 (2002).
- [4] O. Schiemann and T. F. Prisner, *Q. Rev. Biophys.* **40**, 1 (2007).
- [5] (a) R. E. Martin, M. Pannier, F. Diederich, V. Gramlich, M. Hubrich, and H. W. Spiess, *Angew. Chem. Int. Ed.* **37**, 2833 (1998). (b) M. Pannier, S. Veit, A. Godt, G. Jeschke, and H. W. Spiess, *J. Magn. Reson.* **142**, 331 (2000).
- [6] A. Weber, O. Schiemann, B. Bode, and T. F. Prisner, *J. Magn. Reson.* **157**, 277 (2002).
- [7] M. Bennati and T. F. Prisner, *Rep. Prog. Phys.* **68**, 411 (2005).
- [8] V. P. Denysenkov, T. F. Prisner, J. Stubbe, and M. Bennati, *Proc. Natn. Acad. Sci. U.S.A.* **103**, 13386 (2006).
- [9] A. Godt, M. Schulte, H. Zimmermann, and G. Jeschke, *Angew. Chem. Int. Ed.* **45**, 7560 (2006).
- [10] Y. Polyhach, A. Godt, C. Bauer, and G. Jeschke, *J. Magn. Reson.* **185**, 118 (2007).
- [11] A. Schweiger and G. Jeschke, *Principles of Pulse Electron Paramagnetic Resonance* (Oxford University Press, Oxford, 2001).
- [12] Note that the peak-to-peak distance corresponds to  $2D_{dip}$  and the edge-to-edge distance to  $4D_{dip}$  in Fourier-transformed PELDOR spectra.
- [13] A. D. Milov, A. G. Maryasov, and Y. D. Tsvetkov, *Appl. Magn. Reson.* **15**, 107 (1998).
- [14] (a) G. Jeschke, G. Panek, A. Godt, A. Bender, and H. Paulsen, *Appl. Magn. Reson.* **26**, 223 (2004). (b) Y.-W. Chiang, P. P. Borbat, and J. H. Freed, *J. Magn. Reson.* **172**, 279 (2005).
- [15] (a) B. E. Bode, D. Margraf, J. Plackmeyer, G. Dürner, T. F. Prisner, and O. Schiemann, *J. Am. Chem. Soc.* **129**, 6736 (2007). (b) O. Schiemann, N. Piton, J. Plackmeyer, B. E. Bode, T. F. Prisner, and J. W. Engels, *Nat. Protoc.* **2**, 904 (2007).
- [16] G. Jeschke, A. Bender, H. Paulsen, H. Zimmermann, and A. Godt, *J. Magn. Reson.* **169**, 1 (2004).
- [17] B. L. Farmer, B. R. Chapman, D. S. Dudis, and W. W. Adams, *Polymer* **34**, 1588 (1993).